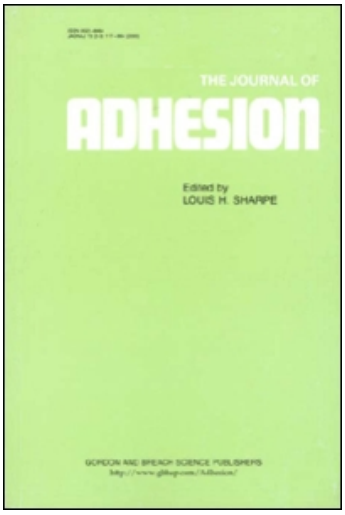

The Journal of Adhesion

Publication details, including instructions for authors and subscription information:
http://www.informaworld.com/smpp/title~content=t713453635

An Improved Procedure for Determining the Work of Adhesion for Polymer-Solid Contact

Pearl Chin[a]; Roy L. McCullough[a]; Wen-Li Wu[b]
[a] Department of Materials Science, University of Delaware, Newark, DE, USA [b] National Institute of Standards and Technology, Polymers Division, Gaithersburg, MD, USA

To cite this Article Chin, Pearl , McCullough, Roy L. and Wu, Wen-Li(1997) 'An Improved Procedure for Determining the Work of Adhesion for Polymer-Solid Contact', The Journal of Adhesion, 64: 1, 145 — 160
To link to this Article: DOI: 10.1080/00218469708010536
URL: http://dx.doi.org/10.1080/00218469708010536

J. Adhesion, 1997, Vol. 64, pp. 145–160
Reprints available directly from the publisher
Photocopying permitted by license only

An Improved Procedure for Determining the Work of Adhesion for Polymer-Solid Contact*

PEARL CHIN[a], ROY L. McCULLOUGH[a,**] and WEN-LI WU[b]

[a]*Department of Materials Science, University of Delaware, Newark, DE, 19713, USA;*
[b]*National Institute of Standards and Technology, Polymers Division, Gaithersburg, MD, 20899 USA*

(Received 7 October 1996; In final form 17 March 1997)

Force-balance experiments in conjunction with the Johnson-Kendall-Roberts (JKR) theory have been used to determine the work of adhesion between solid systems. It has been shown that deficiencies in understanding the deformation behavior can lead to erroneous results. A modified procedure for determining the work of adhesion by force-balance experiments and JKR theory using normal displacement behavior has been introduced to address these deficiencies. This procedure involves improved experiental and data analysis protocols and has been applied to give more precise work of adhesion values for PDMS poly(dimethylsiloxane)-PDMS, PDMS-F(fluorinated silicon) and PDMS-Si (silicon) systems. The work of adhesion determinations are consistently less than those estimated by contact angle measurements.

Keywords: JKR; force-balance;displacement; solid work of adhesion; solid surface energy; PDMS

INTRODUCTION

The determination of the thermodynamic work of adhesion between solid bodies in contact is an important quantity that can impact materials design through prediction of adhesive and interfacial performance. Contact-angle measurements have traditionally been used to

*One of a Collection of papers honoring Yuri S. Lipatov on the occasion of his 70th birthday, 10 July 1997.

**Corresonding author.

estimate the work of adhesion using combining rules for solid-liquid systems. However, a direct measurement of the work of adhesion for solid-solid contact can be achieved with the Johnson-Kendall-Roberts (JKR) force-balance technique [1]. The JKR force-balance device has gained significant attention in recent years by supplying contact area data that can be used to extract adhesion energies.

In this approach [2], a low elastic modulus material in the shape of a hemispherical or spherical lens is brought into contact with a solid surface of interest and the resultant contact area is monitored as a function of applied loading. The contact area is found to vary with applied loading according to the JKR equation, which describes the system behavior as a function of system geometry, material properties and adhesion forces. The low elastic modulus material of primary choice is a crosslinked poly (dimethylsiloxane) (PDMS) network. This material is transparent so that the contact area can be monitored with standard optical microscopes. The system geometry, in this case the radius of curvature of the PDMS hemisphere, is expected to be independently determined. The relative simplicity and convenience of this device is a major factor in its wide-range attraction.

This paper introduces and addresses certain experimental limitations associated with the standard force-balance technique. Methods will be introduced to overcome these limitations for better interpretation of data obtained from the force-balance device.

BACKGROUND

The JKR theory [1] was derived from the Hertz [3] theory of contact mechanics of solid spheres with extensions to account for attractive surface forces *via* an energy balance approach. Linear-elastic, small-strain, and frictionless behavior is assumed. A schematic of the force-balance experiment is shown in Figure 1. The JKR theory describes the system equilibrium between surface and elastic forces *via* the relationship between the contact area and the load, geometry, material properties of the system and surface interactions given by:

$$a^3 = \frac{R}{K}\left\{P + 3\pi W_a R + \sqrt{6\pi W_a R P + 9\pi^2 W_a^2 R^2}\right\} \tag{1}$$

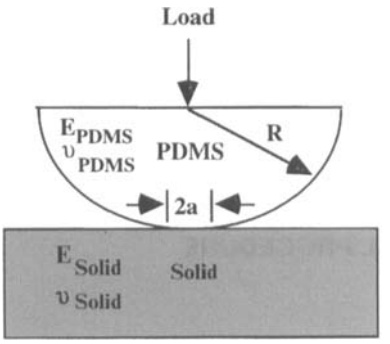

FIGURE 1 Force-balance schematic of PDMS hemisphere on flat surface.

where

$$\frac{1}{K} = \frac{3\pi}{4}(k_1 + k_2) \tag{2}$$

with

$$k_i = \frac{(1 - \upsilon_i^2)}{\pi E_i}$$

where a is the contact radius, P is the applied load, R is the radius of the sphere (or hemisphere), E_i is the elastic modulus of the i'th solid, υ_i is Poisson's ratio of solid i, K is the system modulus and W_a is the work of adhesion of the system. The JKR theory is valid for low elastic modulus systems. Typically, a crosslinked PDMS system is used to meet this requirements.

Monitoring contact radius with applied load with an independent determination of R, previous researchers have implemented a two-parameter least squares fit for material properties w_a and K [2, 4–6] with repeated runs using the same PDMS sample. This data reduction scheme has been generally accepted as the standard data-analysis protocol. However, experimental limitations have not been assessed fully for the force-balance experiment. In the following sections, an analysis of the experimental results for a basic PDMS hemisphere on PDMS flat system will be analyzed and a new experimental protocol developed.

All experiments were performed in a low humidity environment at approximately 5% RH and room temperature, $T \sim 23°C$. The new protocol willbe applied to PDMS in contact with silicon and a fluorinated silicon surface.

EXPERIMENTAL PROCEDURE

Materials

Silicon surfaces analyzed were from single crystal Si slabs. Prior to experiments in the low humidity environment, Si surfaces were pretreated by overnight immersion in sulfuric acid, rinsed with distilled water and air-dried before a subsequent 10 minute, 300 W oxygen plasma treatment and 5-minute treatment with a UV ozone cleaner. Fluorinated surfaces were obtained by 24–48 hour immersion in 0.4% fluorinated trichlorosilane (1H, 1H, 2H, 2H-perfluorodecyl-trichlorosilane ($Cl_3Si(CH_2)_2(CF_2)_7CF_3$)) in carbon tetrachloride soultion [7]; Si substrates were necessary to maintain a reflective surface for monitoring by optical microscopy in reflection mode. Fluorosilane was obtained from PCR, Inc. [8]

PDMS Preparation

Hemispherical PDMS samples were prepared from a mixture of commercial crosslinking PDMS reactants formed on a fluorinated glass slide according to the methods described by Chaudhury [2]. After crosslinking, three additional solvent soaks in fresh methylene chloride (CH_2Cl_2) were implemented to remove uncrosslinked PDMS chains from the system; chloroform can be used as an alternative solvent [9]. Excess free chains migrate to the surface; also, their presence on the surface can affect future surface modifiation attempts. The presence of these chains after recommended solvent extractions was detected during subsequent static contact angle experiments; the static contact angles on PDMS decreased dramatically after only a few seconds. An additional one-hour heat treatment at 250° C in vacuum was necessary to volatilize the excess chains in the system. The final heat treatment was found to be necessary to minimize remaining

PDMS still found to be present even after the solvent extraction steps; the static contact angles on these PDMS surfaces did not change significantly.

Force-Balance Device:

The force-balance device was modifed by the addition of a fiberoptic displacement sensor as in the schematic diagram shown in Figure 2. This force-balance device has been configured for fixed loading conditions (compared with the standard fixed-displacement mode) to allow direct loading and total normal displacement determinations. An optical microscope in reflection mode was connected to a video camera recording system through the objective lens. In this configuration, the flat solid surface of interest must be able to reflect light.

Contact Angles

Contact angles were measured using a Ramé-Hart Contact Angle Goniometer Model 100 [8]. Surfaces were studied using methylene

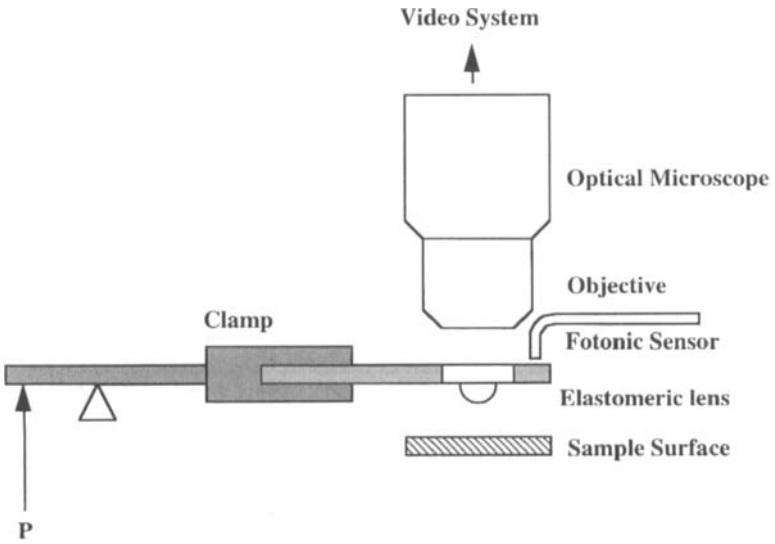

FIGURE 2 Modified force-balance experiment configuration.

iodide (CH_2I_2) and deionized water (DI H_2O). Methylene iodide is largely dispersive and deionized water is largely polar. Static contact angles were measured within 10 seconds of contact with a surface.

RESULTS AND DISCUSSION

The contact radius cubed, a^3, is plotted against the applied load, P, in Figure 3 for a PDMS hemisphere, $R = 1.398$ mm, and PDMS flat, approximately 1.5 mm thick. Applied loading rates were found not to affect observed contact areas and thus were not monitored. The data are fitted for W_a and K by using a nonlinear least squares fitting protocol. The maximum applied load for these experiments is approximately 0.0075 N (750 dynes). The results of this fit give $W_a = 36.4 \pm 1.2 \times 10^{-3}$ J/m^2 (36.4 ± 1.2 ergs/cm^2) and $K = 7.26 \pm 0.06 \times 10^{-1}$ MPa ($7.26 \pm 0.06 \times 10^6$ dynes/cm^2). The uncertainties attached to fitted W_a and K values are

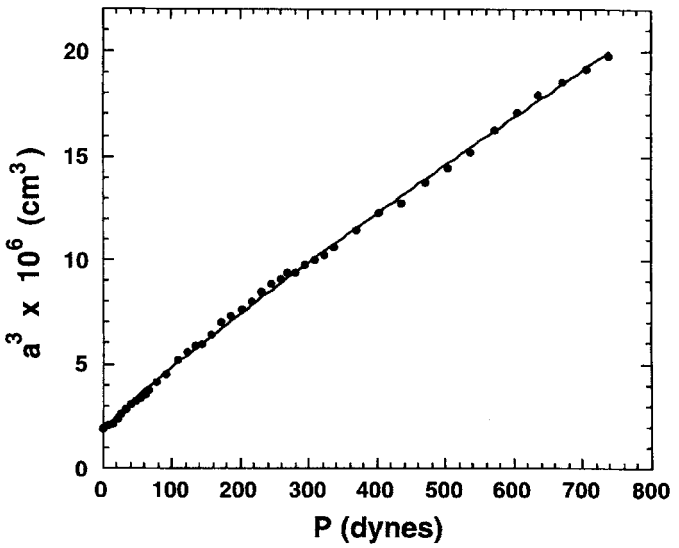

FIGURE 3 JKR standard analysis fit of experimental contact radius a^3 *versus* load P data of PDMS-PDMS system for sample D13A with $R = 1.378$ mm at 5.5% RH and 22.7°C. For these data $W_a = 36.4 \pm 1.2 \times 10^{-3}$ J/m^2 (36.4 ± 1.2 ergs/cm^2); and $K = 7.26 \pm 0.06 \times 10^{-1}$ MPa (7.26 ± 0.06 dynes/cm^2) with $\chi^2 = 1.3262$ and a correlation coefficient of $R = 0.99964$.

the standard error of fitted w_a and K. If data at $P < 0.002$ N (200 dynes) are used, as for results reported for a similar system [2], the resultant fit is $W_a = 31.0 \pm 1.5 \times 10^{-3}$ J/m^2(31.0 ± 1.5 ergs/cm^2) and $K = 6.77 \pm 0.14 \times 10^{-1}$ MPa ($6.77 \pm 0.14 \times 10^6$ dynes/cm^2). The results from the standard JKR analysis for various R systems are compared in Table I for the full load range and in Table II, for fits restriced to $P < 0.002$ N(200 dynes). The uncertainties expressed in the averaged values are the standard deviation of the results. All fits result in correlation coefficients $R > 0.99$. The significant differences in the results due to the choice of loading ranges is evident. In additon, the apparent variability of W_a and K with specimen radius is troublesome, as W_a should be a material property independent of size or loading geometries.

A viable explanation for this anomalous behavior can be attributed to possible violations of the initial assumptions of linear-elastic, small-strain, and frictionless behavior for the derivation of the JKR equation. The crosslinked PDMS system is an elastomer which deforms, initially, linear-elastically. However, the elastic modulus of an elastomer is not necessarily constant with loading, hence dK/dP may not be equal to zero outside of a proper load range. The JKR equation is

TABLE I Standard JKR fit results for PDMS-PDMS Full Range

Sample	R_0 *(mm)*	$W_{a\,fit} \times 10^{-3}$ *(J/m^2)*	$K_{fit} \times 10^{-1}$ *(MPa)*
D13A	1.378	36.4 ± 1.2	7.26 ± 0.06
D16A	1.413	44.8 ± 0.8	7.82 ± 0.04
D8A	2.112	39.5 ± 1.2	7.03 ± 0.07
D15A	2.490	45.2 ± 0.8	7.02 ± 0.05
Average		41.5 ± 3.7	

TABLE II Standard JKR fit results for PDMS-PDMS ($P \leq$ 0.002 N)

Sample	R_0 *(mm)*	$W_{a\,fit} \times 10^{-3}$ *(J/m^2)*	$W_{fit} \times 10^{-1}$ *(MPa)*
D13A	1.378	31.0 ± 1.5	6.77 ± 0.14
D16A	1.413	45.8 ± 1.3	7.88 ± 0.11
D8A	2.112	45.5 ± 1.4	7.65 ± 0.14
D15A	2.490	45.9 ± 1.6	7.13 ± 0.15
Average		42.1 ± 6.4	

more sensitive to surface forces in the low load ranges. Data points from the nonlinear range may cause data-fitting algorithms to assign artificially more weight to the data in the nonlinear range which can result in false W_a determination. The lack of loading guidelines and the variety of maximum loading conditions employed by current researchers for similar size systems indicates that a closer inspection of the validity of the data analysis is necessary. Additionally, lateral deformation is neglected in the derivation of the JKR equation [1]. This assumption may not be valid in the larger strain ranges possible for an elastomeric system, so the instantaneous R may differ significantly from the measured radius of curvature, R_0: *i.e.* $R \neq R_0$. Other sources of nonlinear behavior may be finite size effects [10] or friction.

An analysis of the JKR equation has shown that only two independent parameters can be extracted from a nonlinear least squares fit [11], which initially supports the validity of the current data analysis protocol. However, if the load is such that $R \neq R_0$ due to large lateral deformations or $dK/dP \neq 0$, these additional unknown parameters can then lead to erroneous values for W_a and K from such a fit.

To complicate matters, the possibility of numerous acceptable fits within the experimental measurement error was also observed. Four different W_a and K pairs are listed in Table III which provide satisfactory fits within the measurement error of cubed experimental contact radius data, a^3; these fits were obtained by holding K constant at several physically-feasible values. From this example, although mathematically acceptable, the W_a and K fit corresponding to minimum χ^2 may not be physically representative of the system as there are other W_a and K fits that are acceptable within the experimental error, with difficulty in distinguishing between them. Although not shown here, this phenomenon occurs due to the existence of a shallow minimum in

TABLE III Four acceptable fit results within experimental error for PDMS-PDMS sample D13A, $R = 1.378$ mm

$W_{a\,fit} \times 10^{-3}$	$K_{fit} \times 10^{-1}$
31.5	7.00
36.4	7.26
40.8	7.50
47.6	7.85

χ^2 for W_a and K combinations. This example demonstrates the sensitivity of the least squares fit and χ^2 to random fluctuations in the data. The lack of an independent determination for K becomes an important issue; K must be determined more accurately before W_a can be extracted.

To overcome these problems, additional information in the form of a measurable parameter must be incorporated for proper data reduction. Such a parameter can be the normal displacement, δ, also defined as the displacement of points far away from the contact region. The displacement relationship [1] is given by

$$\delta = \frac{a^2}{3R} + \frac{2P}{3aK} \tag{4}$$

Where the symbols are as defined previously. The use of the displacement measurement and relationship is of recent interest [10–12].

This relation may be rearranged to give

$$\left(\frac{3\delta}{a^2}\right) = \frac{1}{R} + \frac{2}{K}\left(\frac{P}{a^3}\right) \tag{5}$$

This simulataneous measurement, along with contact radius, a, and load, P, can be used to construct a linear plot of $y=(\frac{3\delta}{a^2})$ *versus* $x=(\frac{P}{a^3})$ with slope $2/K$ and intercept $1/R$ since K and R are expected to be constant. A plot in this form has several important features: i) any deviations from linearity can be attributed to violations of $R \cong R_0$ or $dK/dP=0$, so that values for the limiting pressure, P_{cutoff}, can be obtained for use in the standard JKR data reductions; ii) for $P < P_{\text{cutoff}}$, such plots should yield parallel lines if K is constant between specimens; iii) the intercept value can be used to check for $R \cong R_0$. From this data-plotting protocol, the onset of nonlinear behavior at P_{cutoff} can be ascertained and the valid data range can then be chosen for analysis. A direct determination of K from this plot is not recommended due to the large propagated experimental errors from the combination of parameters. The K determination will be addressed in a later section. To make efficient use of the displacement relation, it is necessary to obtain experimental displacement data simulataneously with the contact radii and applied loading data.

The experimental displacement data for PDMS-PDMS in shown in Figure 4. The plot of $3\delta/a^2$ *versus* P/a^3 for the corresponding PDMS-PDMS system is shown in Figure 5.

The displacement relationship in conjunction with the JKR equation can give refined estimates for W_a as well as K. To accomplish these determinations, the simulataneous sum of the deviations from the JKR equation and the displacement relation, given by

$$\Omega^2 = \sum_i \{[a^3(W_a, K, R) - a_i^3] + [\delta(a, k, R) - \delta_i]^2\} \tag{6}$$

must be minimized for data restricted to $P \leqslant P_{\text{cutoff}}$. This fitting protocol involves a global minimization of the fit deviations from the data and reduces the sensitivity to contact radii data fluctuations; DATAPLOT, a linear regression data-fitting software from NIST was used to implement this new fitting protocol [13]. This new fitting method allows a direct, independent K determination since the displacement

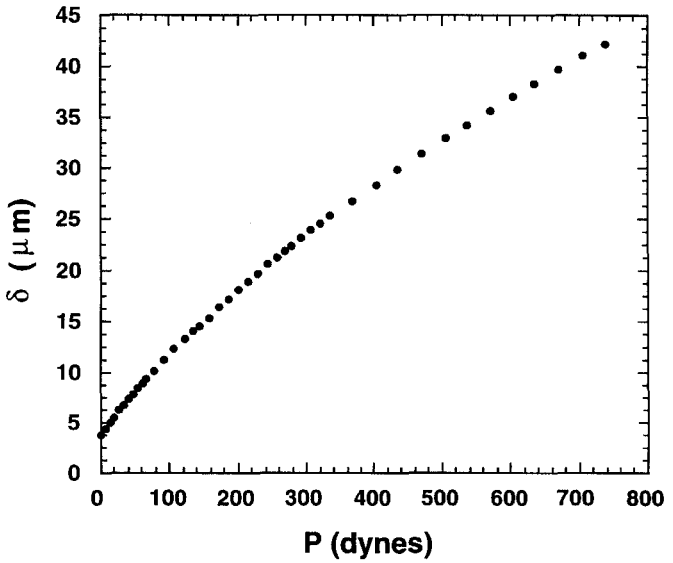

FIGURE 4 Experimental displacement, δ, *versus* load P for PDMS-PDMS system for sample D13A with R = 1.398 mm at 5.5% RH and 22.7°C.

equation has only K as an explicitly undetermined parameter. The results from using this data analysis protocol are shown in Table IV along with P_{cutoff}. The distinct change in the slope of Figure 5 suggests the onset of non-linearity, establishing a value for P_{cutoff} of 0.0019 N (190 dynes). The data in the "Standard" column were obtained by fitting Eq. (1) to the data restricted to $P < P_{cutoff}$. The data in the

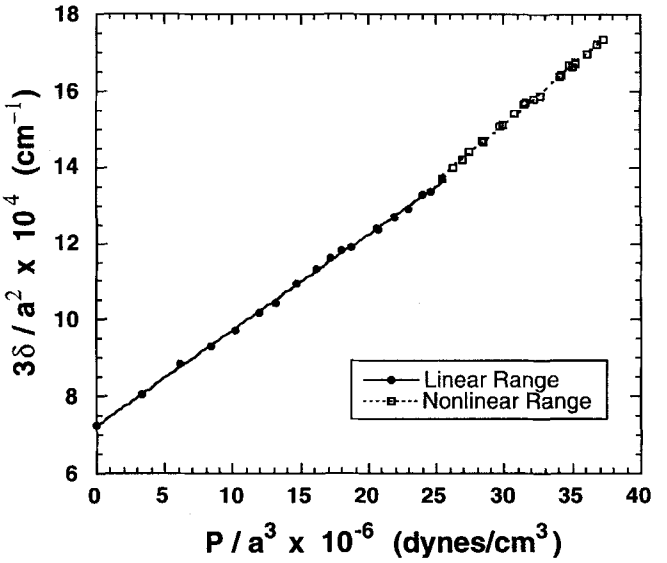

FIGURE 5 Linear fit of $3\delta/a^2$ *versus* P/a^3 with 2 distinct regions for PDMS-PDMS system sample D13A with $R = 1.397$ mm at 5.5% RH and 22.7°C.

TABLE IV PDMS-PDMS New DATAPLOT Simulataneous Fit Results Compared with Standard Fit Results for $P < P_{cutoff}$

Sample	R_0 *(mm)*	$W_{a\,fit} \times 10^{-3}$ *(J/m²) Standard*	$W_{a\,fit} \times 10^{-3}$ *(J/m²) New*	$K_{fit} \times 10^{-1}$ *(MPa) New*	$P_{cutoff} \times 10^{-5}$ *(N)*
D13A	1.378	31.0 ± 1.5	39.8 ± 0.90	7.64 ± 0.09	190
D16A	1.413	45.8 ± 1.3	43.3 ± 0.60	7.60 ± 0.05	160
D8A	2.112	45.5 ± 1.4	38.5 ± 0.60	6.98 ± 0.04	640
D15A	2.490	45.9 ± 1.6	38.0 ± 0.94	6.58 ± 0.06	742*
Average		42.1 ± 6.4	39.9 ± 2.1		

*The asterisk denotes that there is no P_{cutoff} in this range

"New" column were obtained by minimizing Eq. (6) also restricted to $P < P_{\text{cutoff}}$. The utilization of the additional displacement data improves the consistency for values of W_a. The precision of the W_a determinations is greatly improved and resultant W_a is independent of R. A decreasing trend in K with increasing R is observed.

The PDMS-PDMS system is an example of compliant solid systems, but, in practice, a rigid solid surface for at least one of the systems would be more common. The new experimental protocols were applied to a relatively low and high adhesion system to demonstrate the sensitivity of the new methods: PDMS-F and PDMS-Si systems. A single crystal Si wafer and a fluorinated Si wafer were used as the relatively high and low energy surfaces of interest. The results obtained from the improved force-balance experiment are shown in Tables V and VI. For PDMS-F and PDMS-Si systems, the measured W_a were found to be $29.8 \pm 0.6 \times 10^{-3}$ J/m^2 (29.8 ± 0.6 ergs/cm^2) and $59.0 \pm 2.1 \times 10^{-3}$ J/m^2 (59.0 ± 2.1 ergs/cm^2), respectively. Again, the precision indicated by the decreased standard deviation of the average W_a is greatly improved over the standard JKR data analysis. Differences in W_a results between a simple PDMS surface and relatively low-and high-energy surfaces, F and Si, respectively, are clearly distinguishable.

TABLE V Comparison of Data-Analysis Results for PDMS-F

Sample	R_0 *(mm)*	$W_{a\,fit} \times 10^{-3}$ *(J/m²) Standard*	$K_{fit} \times 10^{-1}$ *(MPa) Standard*	$W_{a\,fit} \times 10^{-3}$ *(J/m²) New*	$K_{fit} \times 10^{-1}$ *(MPa) New*	$P_{cutoff} \times 10^{-5}$ *(N)*
F131	1.638	32.8 ± 1.9	14.84 ± 0.23	30.6 ± 1.0	14.79 ± 0.16	200
F41	1.704	29.4 ± 0.7	15.38 ± 0.09	29.9 ± 0.6	15.25 ± 0.08	240
F151	2.061	42.4 ± 1.4	17.38 ± 0.18	29.0 ± 1.0	14.76 ± 0.13	370
F141	2.122	44.5 ± 1.1	16.23 ± 0.13	29.7 ± 1.5	13.26 ± 0.22	400
Average		37.3 ± 6.4		29.8 ± 0.6		

TABLE VI Comparison of data-analysis results for PDMS-Si

Sample	R_0 *(mm)*	$W_{a\,fit} \times 10^{-3}$ *(J/m²) Standard*	$K_{fit} \times 10^{-1}$ *(MPa) Standard*	$W_{a\,fit} \times 10^{-3}$ *(J/m²) New*	$K_{fit} \times 10^{-1}$ *(MPa) New*	$P_{cutoff} \times 10^{-5}$ *(N)*
S14A	1.531	42.8 ± 1.5	13.17 ± 0.13	57.6 ± 1.4	15.01 ± 0.10	470
S11D	2.571	44.8 ± 2.0	11.68 ± 0.20	58.5 ± 2.4	14.29 ± 0.42	600
Average		43.8 ± 1.0		58.1 ± 0.5		

In light of these results, it is of interest to compare the work of adhesion estimated from direct solid-solid contacts with those estimates obtained from solid-liquid contact. Solid surface energies have been commonly estimated from contact angle measurements from solid-liquid theory based on the geometric or harmonic mean relationships of the dispersive and polar components.
From Young's equation, given by

$$\gamma_{lv}\cos\theta = \gamma_{sv} - \gamma_{sl} \tag{7}$$

and the work of adhesion, W_{av}, of separating the solid-liquid interface in the presence of the vapor of the liquid,

$$W_{av} = \gamma_{sv} + \gamma_{lv} - \gamma_{sl} \tag{8}$$

yields

$$W_{av} = \gamma_{lv}(1+\cos\theta) \tag{9}$$

where γ_{lv} is the surface energy of the liquid in equilibrium with its vapor, γ_{sv} is the surface energy of the solid in equilibrium with the vapor of the liquid, and γ_{sl} is the surface energy of the solid in equilibrium with the liquid. Measurement of the contact angles of the surfaces with methylene iodide and deionized water provide the information to estimate γ_s^d and γ_s^p for the surface of interest according to either the geometric [13–16] or harmonic [15–18] mean approximation, depending upon the nature of the surfaces involved; *viz.*

$$\sqrt{\gamma_s^d\,\gamma_{lvi}^d} + \sqrt{\gamma_s^p\,\gamma_{lvi}^p} = \gamma_{lvi}\cos^2(\theta_i/2) \tag{10}$$

or

$$\frac{2\gamma_s^d\gamma_{lvi}^d}{\gamma_s^d+\gamma_{lvi}^d} + \frac{2\gamma_s^p\gamma_{lvi}^p}{\gamma_s^p+\gamma_{lvi}^p} = \gamma_{lvi}\cos^2(\theta_i/2), \tag{11}$$

with $i=1, 2$. Application of the geometric and harmonic mean approximations to the materials of interest in this study are presented in Table VII.

TABLE VII Comparison of Solid Surface Energies from Methylene Iodide and Water Contact Angles between the Geometric Mean and Harmonic Mean Methods

Material	*Geometric Mean*			*Harmonic Mean*		
	γ_s *(ergs/cm)*^{2}	γ_s^d *(ergs/cm*^{2}*)*	γ_s^p *(ergs/cm*^{2}*)*	γ_s *(eregs/cm*^{2}*)*	γ_s^d *(ergs/cm*^{2}*)*	γ_s^p *(ergs/cm*^{2}*)*
Si	53.5	33.5	20	52.8	29.4	23.4
SiF	10.5	5.3	5.2	16.6	6.0	10.6
PDMS	21.6	7.2	14.4	24.3	8.1	16.2

The work of adhesion between solid surfaces is typically estimated by using these solid surface energies approximated from contact angles either by the geometric mean relationship [13–16],

$$W_a = 2\sqrt{\gamma_\alpha^d \gamma_\beta^d} + 2\sqrt{\gamma_\alpha^p \gamma_\beta^p} n \tag{12}$$

or the harmonic mean [15–18] relation

$$W_a = \frac{4\gamma_\alpha^d \gamma_\beta^d}{\gamma_\alpha^d + \gamma_\beta^d} + \frac{4\gamma_\alpha^p \gamma_\beta^p}{\gamma_\alpha^p + \gamma_\beta^p} \tag{13}$$

The comparison of work of adhesion between solid-liquid estimates and the analyses of direct solid-solid contacts are summarized in Table VIII. In all cases, the directly-determined solid-solid work of adhesion is less than the values estimated from solid-liquid contact.

TABLE VIII Comparison of W_a between Fits by New Data Analysis and Predictions from Solid Liquid Theory

System	$W_{a\,fit} \times 10^{-3}$ *(J/m*^{2}*)*	*Geometric Mean* $W_a \times 10^{-3}$ *(J/m*^{2}*)*	*Harmonic Mean* $W_a \times 10^{-3}$ *(J/m*^{2}*)*
PDMS-PDMS	39.9 ± 2.07	43.2	48.6
PDMS-SiF	29.8 ± 0.6	40.2	39.5
PDMS-Si	58.1 ± 0.5	69.0	83.9

CONCLUSION

The standard force-balance experiment has been shown to exhibit deficiencies. In particular, the onset of nonlinear behavior at earlier than anticipated load ranges can lead to erroneous results. The standard data analysis protocol by the JKR equation has also been shown to be highly sensitive to random data fluctuations. The evolution of a new data-analysis protocol has been presented. The displacement equation is required to help clarify the relationship between a^3, W_a and K. The unique use of the normal displacement relation in this work has provided a method to identify the onset of nonlinear behaviour to give valid data ranges for analysis by the JKR equation. A fiberoptic displacement sensor in a fixed-load configuration was added to allow simultaneous acquisition of displacement and contact radii data. A straightforward, non-linear least sum-of-squares data fitting method is introduced and has been shown to be successful in determining consistent and reproducible W_a values. The new data-analysis protocol results in more accurate,consistent and reproducible W_a determinations between PDMS-PDMS, PDMS-F and PDMS-Si solid-solid systems by force-balance experiments. Work of adhesion estimations using solid-liquid theory do not seem appropriate for solid-solid systems. It has also been shown that fresh surface must be used each time due to the occurrence of irreversible surface damage after contact.

It is of interest to note that the new data analysis protocol indicates a consistent trend of decreased system modulus, K, with increasing radius of curvature, R_0. This behaviour could be due to the formation of a more rigid surface layer of uniform thickness on the polymer hemisphere [19]. This rigid surface layer phenomenon will be addressed in a subsequent report.

References

[1] Johnson, K. L., Kendall, K. and Roberts, A. D., *Proc. R. Soc. London, A.* **324**, 301 (1971).
[2] Chaudhury, Manoj K. and Whitesides, George M., *Langmuir* **7**, 1013–1025 (1991).
[3] Hertz, H., *Miscellaneous Papers*, (Macmillan, London 1896), p. 146.
[4] Chaudhury, Manoj K. and Whitesides, George M., *Science* **225**, 1230–1232 (6 March, 1992).
[5] Chaudhury, Manoj K., *Contact Angle, Wettability and Adhesion,* Mittal, K. L., Ed. (VSP, Utrecht, 1993) pp. 691–697.

[6] Chaudhury, Manoj K. and Owen, Michael J., *J. Phys. Chem.* **97**, 5722–5726 (1993).
[7] Wasserman, Stephen R., Tao, Yu-Tai and Whitesides, George M., *Langmuir* **5**, 1074–1087 (1989).
[8] Certain commercial materials and equipment are identified in this paper in order to specify adequately the experimental procedure. In no case does such identification imply recommendation or endorsement by the National Institute of Standards and Technology, nor does it imply that the items identified are necessarily the best available for the purpose.
[9] Silberzan, Pascal; Perutz, Suzanne; Kramer, Edward J. and Chaudhury, Manoj K., *Langmuir* **10**, 2466–2470 (1994).
[10] Shull, Kenneth, Ahn, Dongchan, and Mowery, Cynthia, submitted to langmuir.
[11] Chin, P., *Characterization of Polymer-solid Adhesion*, Ph.D. Thesis, University of Delaware, August 1996.
[12] Ahn, Dongchan and Shull, Kenneth, *Macromolecules* **29**, 4381–4390, (1996).
[13] Fillibe, James and Heckert, Alan, *Dataplot* Interactive Graphics and Data Analysis Langua, National Institute of Standards and Technology.
[14] Wu, Souheng, *J. Polym. Sci.* **74**, 632 (1970).
[15] Wu, Souheng, *J. Phys. Chem.* **C34**, 19 (1971).
[16] Wu, Souheng, *J. Adhesion* **5**, 39 (1973)
[17] Fowkes, F. M., *Adv. Chem. Ser.* **43**, 99 (1964).
[18] Fowkes, F. M., in *Surfaces and Interfaces*, Burke, John, J., Reed, L., Weiss, Volker, Eds. (Syracuse University Press, Syracuse, 1967), p. 197.
[19] VanLandingham, M. R., McKnight, S. H., Palmese, G. R., Eduljee, R. F. Gillespie, J. W. Jr. and McCullough, R. L., "Relating Elastic Modulus to Indentation Response Using Atomic Force Microscopy", *Proceedings of the Eleventh Conference of the American Society for Composites*, submitted.